JOURNAL OF AGRICULTURAL AND FOOD CHEMISTRY
ARTICLE

J. Agric. Food Chem. **2009,** *57,* 4939–4947 **4939**
DOI:10.1021/jf900804j

CO_2 Volume Fluxes Outgassing from Champagne Glasses in Tasting Conditions: Flute versus Coupe

Gérard Liger-Belair,*,† Sandra Villaume,† Clara Cilindre,†
Guillaume Polidori,§ and Philippe Jeandet†

†Laboratoire d'œnologie et Chimie Appliquée, UPRES EA 2069, URVVC and §Laboratoire de Thermomécanique, Groupe de Recherche en Sciences Pour l'Ingénieur (GRESPI), Faculté des Sciences, Université de Reims, B.P. 1039, 51687 Reims Cedex 2, France

Measurements of CO_2 fluxes outgassing from glasses containing a standard Champagne wine initially holding about 11.5 g L^{-1} of dissolved CO_2 were presented, in tasting conditions, during the first 10 min following the pouring process. Experiments were performed at room temperature, with a flute and a coupe, respectively. The progressive loss of dissolved CO_2 concentration with time was found to be significantly higher in the coupe than in the flute, which finally constitutes the first analytical proof that the flute prolongs the drink's chill and helps it to retain its effervescence in contrast with the coupe. Moreover, CO_2 volume fluxes outgassing from the coupe were found to be much higher in the coupe than in the flute in the early moments following pouring, whereas this tendency reverses from about 3 min after pouring. Correlations were proposed between CO_2 volume fluxes outgassing from the flute and the coupe and their continuously decreasing dissolved CO_2 concentration. The contribution of effervescence to the global kinetics of CO_2 release was discussed and modeled by use of results developed over recent years. Due to a much shallower liquid level in the coupe, bubbles collapsing at the free surface of the coupe were found to be significantly smaller than those collapsing at the free surface of the flute, and CO_2 volume fluxes released by collapsing bubbles only were found to be approximately 60% smaller in the coupe than in the flute. Finally, the contributions of gas discharge by invisible diffusion through the free surface areas of the flute and coupe were also approached and compared for each type of drinking vessel.

KEYWORDS: Champagne; sparkling wines; carbonated beverages; CO_2; effervescence; bubble nucleation; Champagne tasting

INTRODUCTION

From a strictly chemical point of view, Champagne and sparkling wines are multicomponent hydroalcoholic systems supersaturated with CO_2 dissolved gas molecules formed together with ethanol during the second fermentation process. Actually, during this second fermentation process, which occurs in cool cellars, the bottles are sealed, so that the CO_2 molecules cannot escape and progressively dissolve into the wine. Therefore, dissolved CO_2 molecules in the wine and gaseous CO_2 molecules under the cork progressively establish equilibrium (an application of Henry's law, which states that the partial pressure of a given gas above a solution is proportional to the concentration of the gas dissolved into the solution). Champagne or sparkling wines elaborated according to the *méthode traditionnelle* typically hold about 10−12 g/L of dissolved CO_2 molecules (*1*). As soon as a bottle of Champagne or sparkling wine is uncorked, the liquid instantaneously becomes supersaturated with dissolved CO_2 molecules (because ambient air contains only traces of gaseous CO_2). To reach a new stable thermodynamic state with regard to CO_2 molecules, Champagne must therefore progressively degas. The progressive release of CO_2 dissolved gas molecules from the liquid medium is responsible for bubble formation (the so-called effervescence process). It is worth noting that approximately 5 L of gaseous dissolved CO_2 must escape from a typical 0.75 L champagne bottle. It is no wonder Champagne and sparkling wine tasting mainly differs from still noneffervescent wine tasting due to the presence of carbon dioxide bubbles continuously rising through the liquid medium. This is why considerable efforts have been conducted the past few years to better illustrate, detect, understand, and finally control each and every parameter involved in the bubbling process (for a review, see, for example, ref (*2*) and references cited therein). Moreover, it is worth noting that there are indeed two pathways for progressive CO_2 and volatile organic compound (VOC) losses after Champagne is poured into a flute. CO_2 and VOC can escape (i) into the form of bubbles nucleated on the glass wall, the so-called effervescence process, and (ii) by "invisible" diffusion through the free air/Champagne interface (i.e., the free surface of the glass) (*1*, *2*). Glass shape is therefore also suspected to play an important role with regard to the kinetics of CO_2 and flavor release during Champagne tasting (*1*−*3*).

*Corresponding author (telephone/fax + 333 26 91 86 14; e-mail gerard.liger-belair@univ-reims.fr).

 Published on Web 05/06/2009

From the consumer's point of view, the role of bubbling is indeed essential in Champagne, in sparkling wines, and even in any other carbonated beverage. Without bubbles, Champagne would be unrecognizable, and beers and sodas would be flat (*3*−*6*). However, the role of effervescence is suspected to go far beyond the solely aesthetical point of view. Actually, in enology, effervescence is also strongly believed to indirectly play another major role concerning flavor release and CO_2 discharge in glasses holding Champagne and sparkling wines. It was indeed recently demonstrated that the continuous flow of ascending bubbles through the liquid medium strongly modifies the mixing and convection conditions of the liquid medium (*7*−*9*). In turn, the CO_2 discharge by diffusion through the free air/Champagne interface may be considerably accelerated, as well as the release of the numerous volatile (and potentially aromatic) organic compounds, which both strongly depend on the mixing flow conditions of the liquid medium (*10*). A strong coupling therefore finally exists between rising bubbles, glass shape, CO_2 discharge, and flavor release. Otherwise, from the consumer's point of view, the release of a sudden and abundant quantity of CO_2 above the Champagne surface is known to strongly irritate the nose during the evaluation of aromas. Quite recently, glassmakers showed interest in proposing soon to consumers a new generation of champagne tasting glasses, especially designed, with a well-controlled CO_2 release during tasting (*7*). This is why, in recent years, much study has been devoted to better understand and depict each parameter involved in the release of gaseous CO_2 from glasses holding Champagne or sparkling wine. In a recent paper, the role of temperature on the kinetics of CO_2 fluxes outgassing from a champagne flute was investigated (*11*). Very recently, also, the development of a compact CO_2 sensor based on near-infrared laser technology for enological applications was reported (*12*).

In this paper, measurements of CO_2 fluxes outgassing from glasses containing a standard Champagne wine initially holding about 11.5 g L^{-1} of dissolved CO_2 were presented, in tasting conditions, during the first 10 min following the pouring process. Experiments were performed at room temperature with two quite emblematic types of champagne drinking vessels: (i) a classical flute, namely, a long-stemmed glass with a deep tapered bowl and a narrow aperture, and (ii) a classical coupe, namely, a shallower glass with a much wider aperture. The contribution of effervescence (i.e., CO_2 bubbles nucleating, ascending, and finally collapsing at the Champagne surface) to the global kinetics of CO_2 release was discussed and modeled by use of results developed over recent years. The contributions of gas discharge by invisible diffusion through the free surface areas of the flute and coupe were also approached and compared for each type of drinking vessel.

MATERIALS AND METHODS

Some Physicochemical Parameters of Champagne. A standard commercial Champagne wine was used for this set of experiments, namely, a "young" one, recently elaborated (vintage 2007) and stored in a cool cellar since it was elaborated. Some classical physicochemical parameters of Champagne samples were already determined at 20 °C, with samples of Champagne first degassed (*13*). The static surface tension of Champagne, γ, was found to be of the order of 50 mN m^{-1}, its density, ρ, was measured and found to be close to 10^3 kg m^{-3}, and its dynamic viscosity, η, was found to be of the order of 1.5×10^{-3} kg m^{-1} s^{-1} (i.e., 1.5 mPa·s).

Glass-Washing Protocol. To avoid the randomly located "bubbling environment" inevitably provided in glasses showing natural effervescence (*14*), we decided to use, for this set of experiments, single standard flutes and coupes engraved on their bottoms (thus providing a "standardized" and artificial effervescence). A rendering of the ring-shaped engravement releasing bubbles at the bottom of the flute is displayed in **Figure 1**. More details on artificial bubble nucleation provided by laser engravement techniques can be found in ref (*7*). Between the successive pouring and time series data recordings, the flute and the coupe were systematically thoroughly washed in a dilute aqueous formic acid solution, rinsed using distilled water, and then compressed-air-dried. This drastic treatment eliminates the formation of calcium carbonate crystals on the glass wall as well as the adsorption of any dust particle acting as "natural" bubble nucleation sites. Therefore, with such a surface treatment, the CO_2 bubble nucleation is strictly restricted to the bubble nucleation sites of the ring-shaped engravement, so that differences in the kinetics of CO_2 release from one type of drinking vessel to another are attributed only to geometrical differences between them.

Experimental Setup and Procedure Used To Measure the Flux of CO_2 Desorbing from Each Type of Drinking Vessel. A volume of 100 mL of Champagne was carefully poured into the glass to test. Characteristic geometrical dimensions and liquid levels of the flute and coupe once they are filled with 100 mL of Champagne are displayed in **Figure 2**. Immediately after the pouring process, the glass was then manually placed on the weighing chamber base plate of a precision weighing balance (Sartorius, Extend Series ED, Germany) with a total capacity of 220 g and a standard deviation of ±0.001 g. The Sartorius balance was interfaced with a laptop PC recording data every 5 s from the starting signal, activated just before the glass holding Champagne was placed on the weighing chamber base plate. The total cumulative mass loss experienced by the glass holding Champagne was recorded during the first 10 min following the pouring process. Actually, the mass loss of the glass holding Champagne is the combination of both (i) Champagne evaporation and (ii) CO_2 progressively desorbing from the supersaturated liquid. The mass loss attributed to Champagne evaporation only was accessible by recording the mass loss of each type of glass containing a sample of 100 mL of Champagne first degassed under vacuum. Due to likely variations in hygrometric conditions from one day to another (occurring even in a climatized temperature-controlled room), Champagne evaporation was thus measured with a sample of Champagne first degassed under vacuum, just before each series of total mass loss recordings were done. Finally, the cumulative mass loss versus time attributed only to CO_2 molecules progressively desorbing from Champagne may therefore easily be accessible by subtracting the data series attributed to evaporation only from the total mass loss data series.

From a cumulative mass loss−time curve, the total mass flux of CO_2 desorbing from the Champagne surface (denoted F_{CO_2}) is therefore deduced during the degassing process in the flute, by dividing the mass loss Δm between two data recordings by the time interval Δt between two data recordings (i.e., $F_{CO_2} = \Delta m/\Delta t$, Δt being equal to 5 s). In other words, the CO_2 mass flux (in grams per second) desorbing out of the Champagne surface is determined by the slope of the curve drawn by the cumulative CO_2 mass loss data recordings. In Champagne and sparkling wine tasting, it is nevertheless certainly more pertinent to deal with volume fluxes rather than with mass fluxes of CO_2. By considering the gaseous CO_2 desorbing out of the Champagne as an ideal gas, the experimental total volume flux of CO_2 (in m^3 s^{-1}), denoted F_T, is therefore deduced as follows, during the degassing process:

$$F_T = \left(\frac{RT}{MP}\right)\frac{\Delta m}{\Delta t} \quad (1)$$

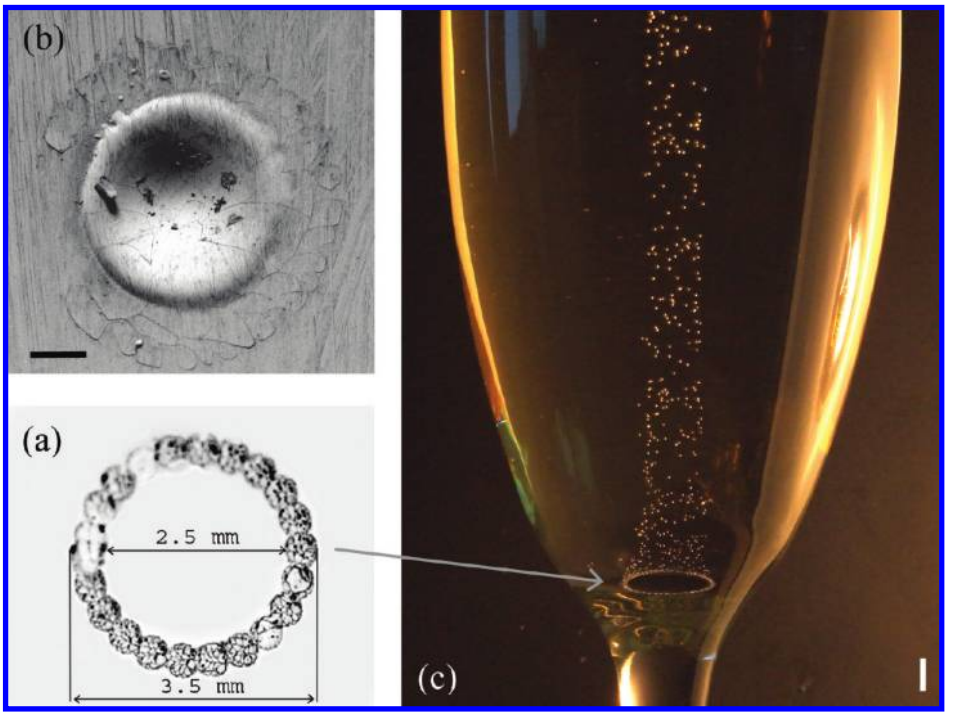

Figure 1. At the bottom of this flute, on its axis of symmetry, the glassmaker has engraved a small ring (done with adjoining laser beam impacts) (**a**); single laser beam impact as viewed through a scanning electron microscope (bar = 100 μm) (**b**); effervescence in this flute is promoted from these "artificial" micro scratches into the form of a characteristic and easily recognizable vertical bubble column rising on its axis of symmetry (**c**) (bar = 1 mm).

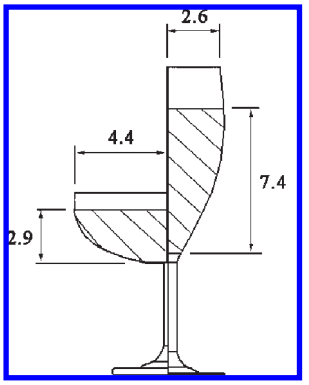

Figure 2. Radii of aperture and liquid levels of the flute (right) and coupe (left) once they are filled with 100 mL of Champagne (characteristic dimensions are indicated in cm).

R is the ideal gas constant (equal to 8.31 J K^{-1} mol^{-1}), T is the Champagne temperature (expressed in K), M is the molar mass of CO_2 (equal to 44 g mol^{-1}), P is the ambient pressure (close to 10^5 N m^{-2}), the loss of mass between two successive data records Δm is expressed in g, and Δt is the time interval between two data recordings (i.e., 5 s in the present case).

To enable a statistical treatment, six successive pouring and time series data recordings were done for each type of drinking vessel (namely, the flute and the coupe). At each step of the time series (i.e., every 5 s), an arithmetic average of the six data provided by the six successive time series corresponding to a given type of drinking vessel finally produce a single "average" time series that is characteristic of a given type of drinking vessel (with standard deviations corresponding to the root-mean-square deviations of the values provided by the six successive data recordings).

Measuring Concentrations of Dissolved CO_2 in Champagne Samples. Concentrations of CO_2 molecules dissolved in Champagne samples were determined using carbonic anhydrase (labeled C2522 Carbonic Anhydrase Isozyme II from bovine erythrocytes and provided from Sigma-Aldrich). This is the official method recommended by the International Office of Vine and Wine (OIV) for measuring the CO_2 content in Champagne and sparkling wines (*15*). This method is thoroughly detailed in a recent paper by Liger-Belair et al. (*11*).

Laser Tomography Technique Used To Visualize the Flow Patterns in Champagne Glasses. The laser tomography workbench and the technique used to visualize the mixing flow patterns found in champagne glasses under various glass-shaped and engravement conditions were already thoroughly detailed in recent papers (*7*−*9*). In the present work, the laser tomography technique used to freeze the Champagne flow patterns was nevertheless slightly modified (and improved) compared to that previously described in the above-mentioned references. Actually, to avoid optical distortions induced by the curved surface of the glass, the latter was immersed in a parallelepipedic tank full of water with a refractive index (n = 1.332) very close to that of Champagne (n = 1.342). Thanks to this slight modification, the quality of snapshots was indeed highly improved compared to the ones found in refs (*7*−*9*).

RESULTS AND DISCUSSION

Initial Concentration of Dissolved CO_2 inside the Bottles, after Uncorking. To enable a statistical treatment, six successive CO_2 dissolved measurements were systematically done on six distinct bottles by use of carbonic anhydrase (just after uncorking a bottle, but before pouring). The Champagne elaborated in 2007 was found to initially hold (before pouring) a concentration of CO_2 dissolved molecules of $[CO_2] = 11.6 \pm 0.3$ g L^{-1}.

Initial Concentration of Dissolved CO_2 in Each Type of Drinking Vessel, after Pouring. As already demonstrated in a previous paper, the pouring process is far from being consequence-less with regard to c_L (*11*). During the several seconds of the pouring process preceding the beginning of the cumulative mass loss−time series, Champagne undergoes highly turbulent and swirling

flows. During this phase, Champagne loses a very significant part of its initial content in dissolved CO_2. Consequently, at the beginning of the time series (i.e., at $t = 0$, after the glass was filled with Champagne and manually placed on the base plate of the precision weighing balance), CO_2 dissolved in Champagne is suspected to be well below 11.6 ± 0.3 g L^{-1} (as chemically measured inside a bottle, after uncorking, but before pouring). In the present work, the initial bulk concentration of dissolved CO_2 after pouring, denoted c_i, was also chemically assessed by using carbonic anhydrase. To enable a statistical treatment, six successive CO_2 dissolved measurements were systematically done for each type of drinking vessel, after six successive pourings (from six distinct bottles). Champagne was found to initially hold (at $t = 0$, after pouring) a concentration of CO_2 dissolved molecules of $c_i^{flute} = 7.4 \pm 0.4$ g L^{-1} in the flute, and $c_i^{coupe} = 7.4 \pm 0.5$ g L^{-1} in the coupe (i.e., approximately 4 g L^{-1} less in both types of drinking vessel after pouring than inside the bottle, before pouring). Therefore, it seems that turbulences of the pouring process cause significant and quite unexpected loss of dissolved CO_2 during Champagne serving. It is worth noting that losses of CO_2 dissolved molecules during the pouring process are of the same order of magnitude whether Champagne is served in the flute or in the coupe, despite a significantly longer pouring process in the case of the flute (mainly due to an excess of foam restricted in the narrower aperture, which forces the taster to pour Champagne into the flute in two or three steps to avoid overflow). This observation first appeared counterintuitive to us. Actually, losses of dissolved CO_2 induced by a longer pouring process in the flute could be counterbalanced by the much larger area offered to CO_2 dissolved molecule escape in the case of the coupe aperture. **Table 1** summarizes the geometrical and analytical pertinent parameters linked with each type of drinking vessel filled with 100 mL of Champagne.

Influence of Each Type of Drinking Vessel on Its Loss of Dissolved CO_2 Concentration with Time. The two "average" cumulative mass loss−time series corresponding to the flute and coupe, respectively, are displayed in **Figure 3**, during the first 10 min following the pouring process. Despite significant standard deviations (mainly attributed to the difficult repeatability of the manual pouring process between the six successive pouring and time series data records conducted for each type of drinking vessel), significant differences appear between the two cumulative mass loss−time curves. It is clear from **Figure 3** that the cumulative mass loss of CO_2 with time is higher when Champagne is served in a coupe than in a flute. In enology, the parameter that characterizes a wine sample with regard to its CO_2 content is its CO_2 concentration, denoted c_L, usually expressed in grams per liter. The progressive loss of CO_2 concentration after Champagne was poured into the glass, expressed in grams per liter and denoted $\Delta c(t)$, may finally be easily assessed by retrieving the mass loss−time curves by using the relationship

$$\Delta c(t) = c_L(t) - c_i = -\frac{m(t)}{V_{glass}} \quad (2)$$

with c_i being the initial concentration of CO_2 dissolved into the Champagne after pouring (at $t = 0$), $m(t)$ being the cumulative mass loss of CO_2 with time expressed in g, and V_{glass} being the volume of Champagne poured into the glass expressed in L (namely, 0.1 L in the present case).

For each type of drinking vessel, the corresponding loss of dissolved CO_2 concentration with time during the first 10 min following pouring is displayed in **Figure 4**. It is clear from **Figure 4** that the progressive loss of dissolved CO_2 concentration with time is significantly higher when Champagne is served in the coupe than in the flute. From the taster's point of view, this observation is of importance for both the visual aspect of Champagne and its "mouthfeel" sensation. Actually, it was recently shown that the higher the concentration of dissolved CO_2 in Champagne, the higher the kinetics of bubble nucleation, the larger the average bubbles' size, and finally the more effervescence in the glass (*13*). Moreover, it is also well-known in Champagne and sparkling wine tasting that the higher the concentration of dissolved CO_2, the higher the "fizzy" sensation when bubbles burst over the tongue (*16*). To the best of our knowledge, this is the first set of analytical results concerning the influence of glass shape on its progressive loss of dissolved CO_2 concentrations with time in tasting conditions, and therefore the first analytical proof that a long-stemmed glass with a deep tapered bowl and a narrow aperture prolongs the drink's chill and helps to retain its effervescence in contrast with a shallower coupe of much wider aperture.

Influence of Each Type of Drinking Vessel on CO_2 Volume Fluxes Outgassing from It. In Champagne and sparkling wine tasting, in addition to the visual aspect of effervescence and mouthfeel—both depending on (among many other parameters) the dissolved CO_2 concentration $c(t)$—another important aspect is the smell or "nose" of the wine, the so-called "bouquet" (*16*−*18*). Effervescence of Champagne and sparkling wines promotes the development of aromas in the headspace above the glass. The myriad bubbles nucleating on the flute's wall and traveling through the wine's bulk considerably enhance the perception of VOC by considerably enhancing exchange surfaces between the wine and the atmosphere, as exposed in a recent paper (*11*). However, each bubble collapsing at the wine's surface inevitably frees its tiny CO_2 volume. Consequently, the inevitable counterpart to the "exhausting" aromas effect attributed to bubbles' exchange surfaces is to progressively bring gaseous CO_2 in the headspace above the wine's surface (*11*). It is indeed well-known that a sudden and abundant quantity of CO_2 may irritate the nose during the evaluation of aromas (*16*).

The analytical parameter that characterizes the progressive release of gaseous CO_2 desorbed from a glass filled with Champagne is the total volume flux of CO_2 escaping from the wine/air interface, as defined in eq 1. The total CO_2 volume fluxes outgassing from each type of drinking vessel filled with 100 mL of Champagne are presented in the graph displayed in **Figure 5**, during the first 10 min following the pouring process. Experimentally, during approximately the first 3 min following the pouring process, it is clear that total CO_2 volume fluxes are significantly higher when Champagne is served in the coupe than in the flute. Nevertheless, this tendency reverses from about 3 until 10 min after pouring, and total CO_2 volume fluxes outgassing from the flute become higher than those outgassing from the coupe (see the inset in **Figure 5**).

In a recent paper, it was demonstrated that the driving force behind the progressive desorption of CO_2 from a glass filled with Champagne was its bulk concentration c_L of dissolved CO_2 (*11*). Therefore, it seemed pertinent to propose a correlation between the CO_2 volume flux outgassing from the glass and the continuously decreasing bulk concentration c_L of dissolved CO_2. To do so, time series data recordings displayed in **Figures 4** and **5** were combined. Time was eliminated so that the CO_2 volume flux outgassing from each type of drinking vessel was plotted as a function of Champagne dissolved CO_2 concentration c_L. Correlations between total CO_2 volume fluxes and dissolved CO_2 concentrations in Champagne are displayed in **Figure 6**, for each type of drinking vessel. It is clear from **Figure 6** that, for a given dissolved CO_2 concentration of Champagne, total CO_2 volume fluxes are significantly higher when Champagne is served in a coupe than when it is served in a flute. Experimental data were fitted with polynomial functions (up to orders enabling

Table 1. Pertinent Parameters Linked with Each Type of Drinking Vessel Filled with 100 mL of Champagne

type of vessel	liquid level after pouring, h (cm)	radius of aperture of the glass, r (cm)	surface area offered to gas discharge, A (cm^2)	initial concentration of dissolved CO_2, c_i (g L^{-1})
flute	7.4	2.6	21.2	7.4 ± 0.4
coupe	2.9	4.4	60.8	7.4 ± 0.5

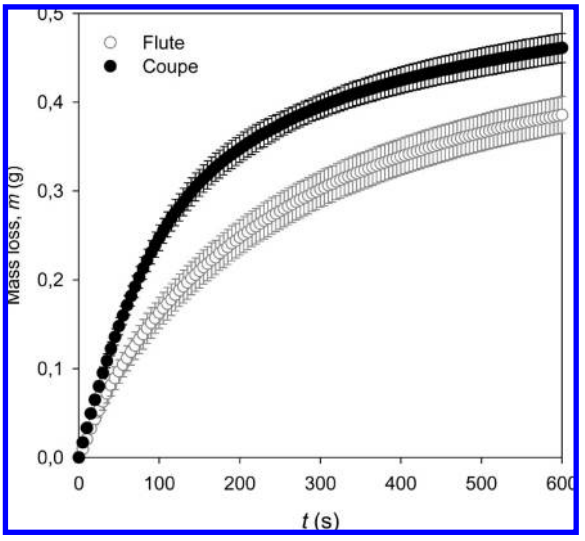

Figure 3. Cumulative mass loss−time series corresponding to the flute and coupe, respectively, during the first 10 min following the pouring process. Each datum point of each cumulative mass loss−time series is the arithmetic average of six successive data issued from six successive pourings; standard deviations correspond to the root-mean-square deviations of the values provided by the six successive data recordings.

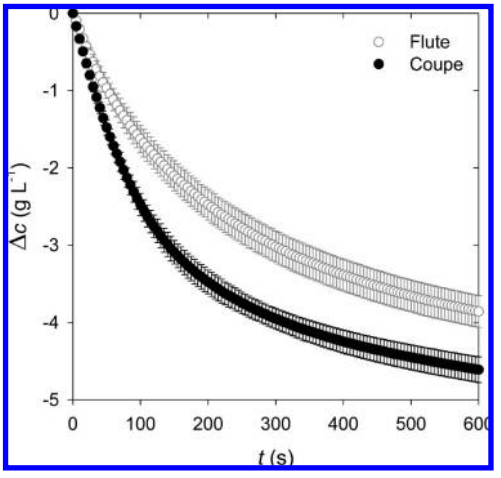

Figure 4. Progressive loss of CO_2 dissolved concentrations (in g L^{-1}) as determined with eq 2 during the first 10 min following the pouring process in a flute and in a coupe, respectively, filled with 100 mL of Champagne. Each datum point of each time series is the arithmetic average of six successive values recorded from six successive pourings; standard deviations correspond to the root-mean-square deviations of the values provided by the six successive data recordings.

correlation coefficients R^2 better than 0.995). Polynomial functions obtained for both the flute and coupe, respectively, are the following:

$$F_T^{\text{flute}} \approx 0.2931 - 0.2242 c_L + 0.0481 c_L^2$$
$$F_T^{\text{coupe}} \approx 1.941 - 1.585 c_L + 0.4006 c_L^2 - 0.0255 c_L^3 \quad (3)$$

From the point of view of Champagne and sparkling wine tasting, the pertinent parameter that characterizes a given type of

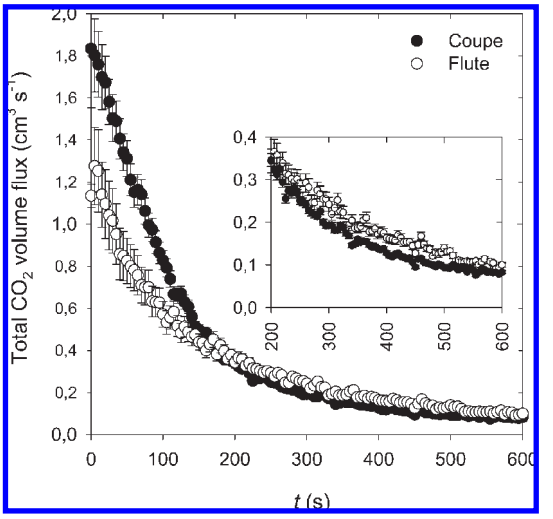

Figure 5. Total CO_2 volume flux recordings (in cm^3 s^{-1}) as determined with eq 1, desorbing from a flute and coupe, respectively, filled with 100 mL of Champagne, during the first 10 min following the pouring process. Each datum point of each time series is the arithmetic average of six successive values recorded from six successive pourings; standard deviations correspond to the root-mean-square deviations of the values provided by the six successive data recordings.

drinking vessel with regard to its progressive CO_2 release with time is not really the total CO_2 volume flux outgassing from it. Actually, the open aperture of tasters' nostrils being obviously much smaller than the surface area of the drinking vessel offered to total gas discharge, we propose a more adapted analytical parameter to compare the progressive CO_2 release from various glasses, namely, the CO_2 volume flux per unit surface area, denoted F_{US}, and deduced as follows for each type of drinking vessel:

$$F_{US} = \frac{F_T}{A} = \frac{1}{A}\left(\frac{RT}{MP}\right)\frac{\Delta m}{\Delta t} \quad (4)$$

A is the free surface area of the given type of drinking vessel (given in **Table 1**). CO_2 volume fluxes per unit surface area outgassing from each type of drinking vessel filled with 100 mL of Champagne are presented in **Figure 7**, during the first 10 min following the pouring process. It is clear from **Figure 7** that CO_2 volume fluxes outgassing per unit surface area are much higher in the flute than in the coupe during the 10 min following the pouring process. From the point of view of Champagne tasting, this means that the flute should finally enable higher concentrations of gaseous CO_2 above the Champagne free surface during the tasting (due to its narrower open aperture compared to that of the coupe), despite the lower total CO_2 volume fluxes in the first 3 min following pouring. Further determination of the gaseous CO_2 concentration above the Champagne free surface, a parameter useful for Champagne tasting, will be soon achieved by the use of gas microchromatography.

Modeling CO_2 Volume Fluxes Outgassing from Each Type of Drinking Vessel: Contribution of Bubbles and the Role of Liquid Level. Actually, the contribution of rising CO_2 bubbles to the

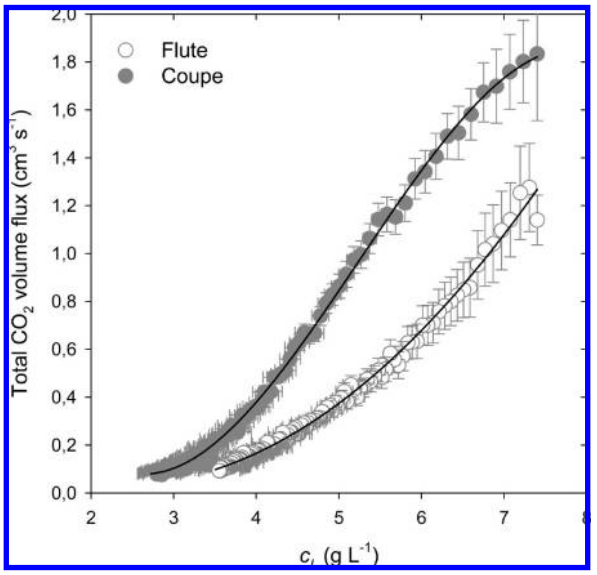

Figure 6. Total CO_2 volume flux recordings (in $cm^3\ s^{-1}$) desorbing from a flute and coupe, respectively, filled with 100 mL of Champagne as a function of their dissolved CO_2 concentration. Each datum point of each time series is the arithmetic average of six successive values recorded from six successive pourings; standard deviations correspond to the root-mean-square deviations of the values provided by the six successive data recordings; experimental data were fitted with polynomial functions, which appear as dashed lines.

global kinetics of CO_2 outgassing from a sparkling beverage is quite easily assessed by taking into account the whole number of nucleation sites found in the glass, the average frequency of bubble production from a nucleation site, and the average size of a bubble as it reaches the liquid surface (to finally collapse and release its CO_2 content in the headspace above the liquid surface). Recently, models based on both classical diffusion and ascending bubble velocity were developed in order to propose scale laws likely to link the frequency of bubble nucleation (i.e., the number of bubbles released per second from a given nucleation site) as well as the size of CO_2 bubbles rising in a carbonated beverage with some physicochemical parameters of the liquid medium. The frequency of bubble formation from a single bubble nucleation site, denoted f and expressed in bubbles per second, was found to obey the scaling law (*19*, *20*)

$$f \approx 5 \times 10^{-8} \frac{T^2(c_L - k_H P)}{\eta P} \quad (5)$$

with T being the liquid temperature (in K), c_L being the bulk concentration of CO_2 in the liquid medium (in g L^{-1}), k_H being the so-called Henry's law constant (i.e, the solubility of the CO_2 molecules with regard to the liquid medium, in g L^{-1} atm^{-1}), P being the ambient pressure (in atm), and η being the liquid dynamic viscosity (in Pa·s).

The diameter of a bubble reaching the liquid surface was also found to depend on various parameters (*2*). Actually, the diameter of a bubble, denoted d and expressed in centimeters, was found to obey the scaling law

$$d \propto 7.3 \times 10^{-3} T^{5/9} \left(\frac{1}{\rho g}\right)^{2/9} \left(\frac{c_L - k_H P}{P}\right)^{1/3} h^{1/3} \quad (6)$$

with ρ being the liquid density (in kg m^{-3}), g being the acceleration due to gravity (in m s^{-2}), and h being the distance traveled by the bubble from its nucleation site (in cm).

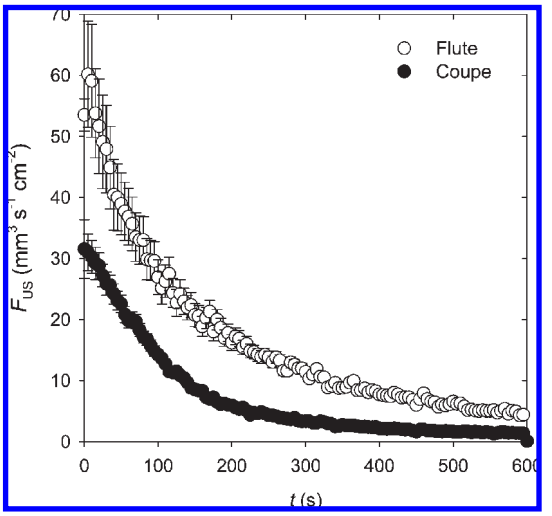

Figure 7. CO_2 volume fluxes per unit surface (in $mm^3\ s^{-1}\ cm^{-2}$) as determined with eq 4, desorbing from a flute and a coupe, respectively, filled with 100 mL of Champagne, during the first 10 min following the pouring process.

It is worth noting from the previous relationship that the only parameter which changes between the coupe and the flute is the liquid level denoted h (every other parameter being equal under the same operating conditions). Therefore, following the previous relationship, the diameter of CO_2 bubbles collapsing at the free surface of a given type of glass is proportional to the one-third power of their traveled distance. The growth of bubbles has also been dealt with recently in the case of ascending Champagne and beer bubbles (*21*), using the more general theoretical development of Zhang and Xu (*22*). More on convective bubble growth and dissolution can be found in a recent textbook by Professor Zhang, wherein some other correlations between the bubble's diameter and its traveled distance (nevertheless quite close to the one expressed by eq 6) are proposed (*23*). The two photographs displayed in **Figure 8** compare the diameters of bubbles as they reach the free surface of the glass, whether Champagne is served in a flute or in a coupe. It is clear from **Figure 8** that the bubble size distribution in both photographs suggests significantly larger bubbles above the free surface of the flute (as expected from eq 6 due to the fact that bubbles travel a longer distance, and finally grow bigger, in the flute than in the coupe).

Finally, the contribution of bubble nucleation to the global CO_2 volume fluxes outgassing from a sparkling beverage may be assessed by multiplying the number N of nucleation sites found in the glass by the average frequency f of bubble nucleation and by the average volume v of a bubble collapsing at the liquid surface. Therefore, by combining the two above-mentioned scaling laws, the CO_2 volume flux released by bubbles rising and collapsing in a carbonated beverage poured into a glass, denoted F_B (and given in $cm^3\ s^{-1}$), obeys the following scaling law:

$$F_B = Nfv \approx \frac{Nfd^3}{2} \approx 9.7 \times 10^{-15} N \frac{T^{11/3}}{\eta} \left(\frac{1}{\rho g}\right)^{2/3} \left(\frac{c_L - k_H P}{P}\right)^2 h \quad (7)$$

It is worth noting from the previous relationship that the only parameter which changes between the coupe and the flute is the liquid level denoted h (every other parameter being equal under the same operating conditions). Therefore, the higher the liquid level, h, the higher the CO_2 volume flux outgassing from the liquid into the form of CO_2 bubbles collapsing at the liquid surface

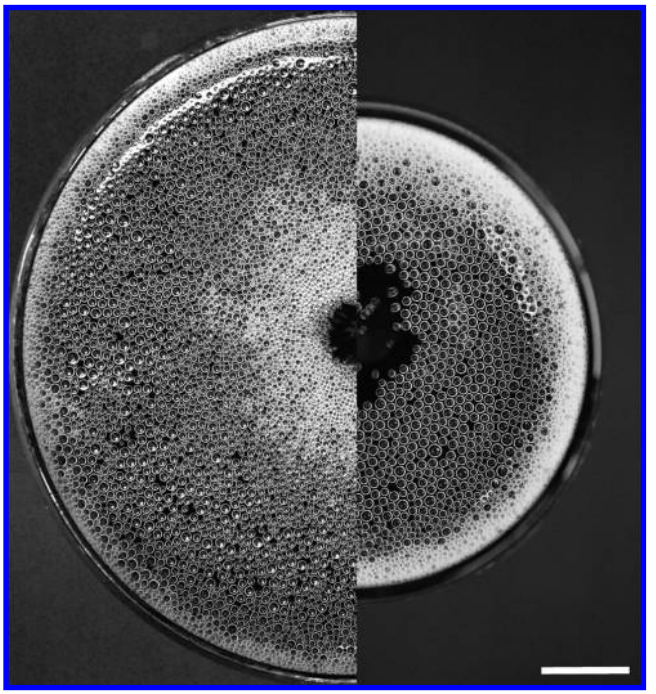

Figure 8. Bubbles' size distribution at the free surface of Champagne, 30 s after pouring, whether Champagne is served in the coupe (left) or in the flute (right) engraved on its bottom. Before the Champagne was poured, the glass-washing protocol was exactly the same as that detailed under Materials and Methods, so that bubbles were generated only from nucleation sites of the ring-shaped engravements (lying, respectively, 2.9 and 7.4 cm below the free surface area, whether Champagne is served in the coupe or in the flute). Bar = 1 cm.

(because CO_2 bubbles grow in size during ascent). CO_2 volume fluxes released by bubbles are thus finally expected to obey the following scaling law:

$$F_B \propto h \tag{8}$$

The previous scaling law teaches us that, for a given type of drinking vessel, CO_2 volume fluxes released by bubbles are simply proportional to the distance h traveled by bubbles. Therefore, the ratio of liquid levels between the coupe and the flute being of the order of $h^{coupe}/h^{flute} \approx 2.9/7.4 \approx 0.4$, CO_2 volume fluxes released by bubbles in the coupe are expected to be of the order of 40% those released by bubbles in the flute, which is expressed as

$$F_B^{coupe} \approx 0.4 F_B^{flute} \tag{9}$$

It is worth noting that, because total CO_2 volume fluxes are finally much higher when Champagne is served in the coupe than in the flute (see **Figure 7**), the previous relationship betrays the fact that CO_2 molecules mostly directly escape by diffusion through the free surface.

Generally speaking, the total CO_2 volume fluxes released from a given vessel filled with Champagne and denoted F_T is the sum of two terms: (i) CO_2 volume fluxes released by bubbles, denoted F_B, and (ii) CO_2 volume fluxes released by diffusion through the free surface area, denoted F_S. Therefore, total CO_2 volume fluxes released from a given vessel are expressed as

$$F_T \approx F_S + F_B \tag{10}$$

The ratio between CO_2 volume fluxes released by diffusion through the free surface area of the coupe and the flute, respectively, may therefore be accessed by retrieving the following relationship:

$$\frac{F_S^{coupe}}{F_S^{flute}} = \frac{F_T^{coupe} - F_B^{coupe}}{F_T^{flute} - F_B^{flute}} \approx \frac{F_T^{coupe} - 0.4F_B^{flute}}{F_T^{flute} - F_B^{flute}} \tag{11}$$

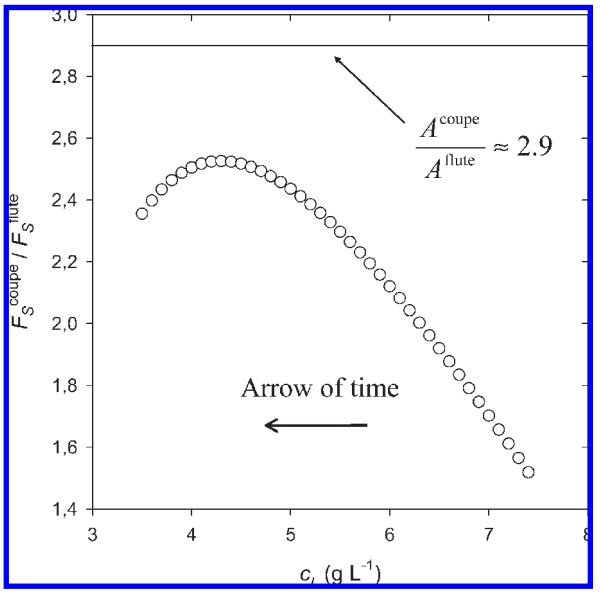

Figure 9. Ratio between CO_2 volume fluxes released by diffusion through the free surface area of the coupe and the flute, respectively, as a function of the decreasing dissolved CO_2 concentration, during the first 10 min after pouring.

The above-defined ratio was plotted in **Figure 9** as a function of the decreasing dissolved CO_2 concentration (during the first 10 min after pouring). F_T^{flute} and F_T^{coupe} were assessed by use of eq 3, and F_B^{flute} was assessed by retrieving in eq 7 each parameter by its numerical value. As shown in **Figure 9**, the ratio F_S^{coupe}/F_S^{flute} shows a very characteristic bell-shaped curve, with a maximum around $F_S^{coupe}/F_S^{flute} \approx 2.5$ found for a dissolved CO_2 concentration of $c_L \approx 4.5$ g L^{-1}.

It is worth noting from **Figure 9** that, very surprisingly, the experimentally determined F_S^{coupe}/F_S^{flute} ratio is always well below the ratio of the surface areas between the coupe and the flute denoted $A^{coupe}/A^{flute} = 60.8/21.2 \approx 2.9$. Intuitively, we had first naively imagined that the ratio of F_S^{coupe}/F_S^{flute} could have been (quite logically) the same as the ratio of surface free areas offered to gas discharge in the coupe and flute, respectively. It is clear from **Figure 9** that it is absolutely not the case. We are therefore logically tempted to wonder why. The last paragraph of the present paper proposes a clue to our preceding interrogation, offered by the fine observation of the flow patterns found in the flute and coupe, respectively, by use of laser tomography techniques.

A Clue Offered by the Observation of Flow Patterns Found Inside Each Type of Drinking Vessel. Molecular diffusion is the mechanism behind the progressive desorption of dissolved gas species from the free surface area of a supersaturated liquid medium (as CO_2 molecules dissolved from the free surface area of the glass). Generally speaking, the desorption of dissolved gas species is ruled by pure diffusion or by diffusion−convection, whether the liquid medium is perfectly stagnant or in motion. In a purely diffusive case, a boundary layer depleted with dissolved gas molecules progressively expands near the free surface area, so that the diffusion of gas species outgassing from the liquid medium inexorably and quickly slows. In the case of a liquid medium agitated with flow patterns, convection forbids the

growing of the diffusion boundary layer by supplying the liquid near the free surface area with dissolved gas molecules freshly renewed from the liquid bulk (*24*). Generally speaking, the higher the velocity of the mixing flow patterns, the thinner the thickness of the diffusion boundary layer and, finally, the higher the volume fluxes of gas species outgassing from the supersaturated liquid medium.

Contrary to the case of a still noneffervescent wine, Champagne served in a flute or a coupe is far from being stagnant during the tasting. Actually, CO_2 bubbles nucleating and detaching from the ring-shaped engravement are driven by buoyancy. As they rise through the liquid medium, bubbles act as exterior shear stresses on the surrounding fluid and induce the formation of large-scale flow patterns, as already shown in previous papers (*7*−*9*). The desorption of CO_2 molecules outgassing from the Champagne free surface area is therefore definitely under the influence of the mixing flow patterns found below the free surface and therefore obeys the laws of diffusion−convection.

Photographs of the flow patterns found inside both types of drinking vessels, as determined by laser tomography techniques, are displayed in **Figure 10**, 3 min after the pouring process. Those two snapshots are very instructive with regard to the way Champagne is mixed in each type of drinking vessel. Significant differences concerning the mixing flow patterns within the Champagne bulk were found between the flute and the coupe. In the case of the coupe, only about half of the liquid medium was found to be mixed by the flow of ascending bubbles arising from the bottom of the coupe. The external periphery of the coupe is characterized by a "dead-zone", where Champagne is almost at rest, contrary to the case of the flute, where the whole liquid bulk was found to be homogeneously mixed up to several minutes after the pouring process. It is clear that the glass shape therefore strongly influences the overall characteristics of mixing flow phenomena found in champagne glasses.

Actually, following the laws of diffusion−convection, and because it is clear from the snapshots displayed in **Figure 10** that the Champagne bulk is not at all identically mixed whether it is served in a flute or in a coupe, it is finally much less surprising to realize that the ratio F_S^{coupe}/F_S^{flute} is completely different from $A^{coupe}/A^{flute} \approx 2.9$. An experimental ratio of $F_S^{coupe}/F_S^{flute} \approx 2.9$ would have been expected in the case of identical mixing conditions in both the flute and the coupe. Due to both a narrow open aperture and a longer distance traveled by bubbles in the flute (which enables them to reach higher rising velocities and therefore higher shear stresses on the surrounding fluid), the Champagne bulk is finally much more vigorously and homogeneously mixed in the flute than in the coupe. It is therefore totally logical to measure ratios F_S^{coupe}/F_S^{flute} well below 2.9, during the first 10 min following the pouring process. A complete explanation of the origin of the bell-shaped curve with a maximum $F_S^{coupe}/F_S^{flute} \approx 2.5$ found for a dissolved CO_2 concentration of $c_L \approx 4.5$ g L^{-1} is nevertheless still under deeper investigation.

In conclusion, measurements of CO_2 fluxes outgassing from a flute and a coupe engraved on their bottoms were conducted during the first 10 min after the pouring of Champagne. The progressive loss of dissolved CO_2 concentrations with time was found to be significantly higher in the coupe than in the flute, which finally constitutes the first analytical proof that the flute prolongs the drink's chill and helps it to retain its effervescence in contrast with the coupe. Moreover, CO_2 volume fluxes outgassing from the coupe were found to be much higher in the coupe than in the flute in the early moments following pouring, whereaas this tendency reverses from about 3 min after pouring. A correlation was proposed between CO_2 volume fluxes outgassing from the flute and the coupe and the continuously decreasing dissolved CO_2 concentration in Champagne. The contribution of bubbles only to the global kinetics of CO_2 release was discussed and modeled by use of results developed over recent years. Due to a much shallower liquid level in the coupe, bubbles collapsing at the free surface of the coupe were found to be significantly smaller than those collapsing at the free surface of the flute. CO_2 volume fluxes released by collapsing bubbles only were found to be approximately 60% smaller in the coupe than in the flute. Finally, the contribution of gas discharge by invisible diffusion only (without the bubbling contribution) was also approached and compared for each type of drinking vessel. Quite counterintuitively, the ratio between CO_2 volume fluxes released by invisible diffusion through the free surface area of the coupe and the flute (without the bubbling contribution) was found to be significantly lower than the ratio of their respective surface free areas. A clue to this unexpected observation was offered by the fine observation of flow patterns found in each type of drinking vessel, which were made visible by laser tomography techniques. This observation betrays much more vigorous mixing phenomena in the flute than in the coupe. Following the law of diffusion−convection, the CO_2 volume flux per unit surface area is therefore expected to be significantly higher through the free surface of the flute than through the free surface of the coupe. A complete mathematical model that includes the multiple pathways of CO_2 discharge during the pouring process is indeed under construction.

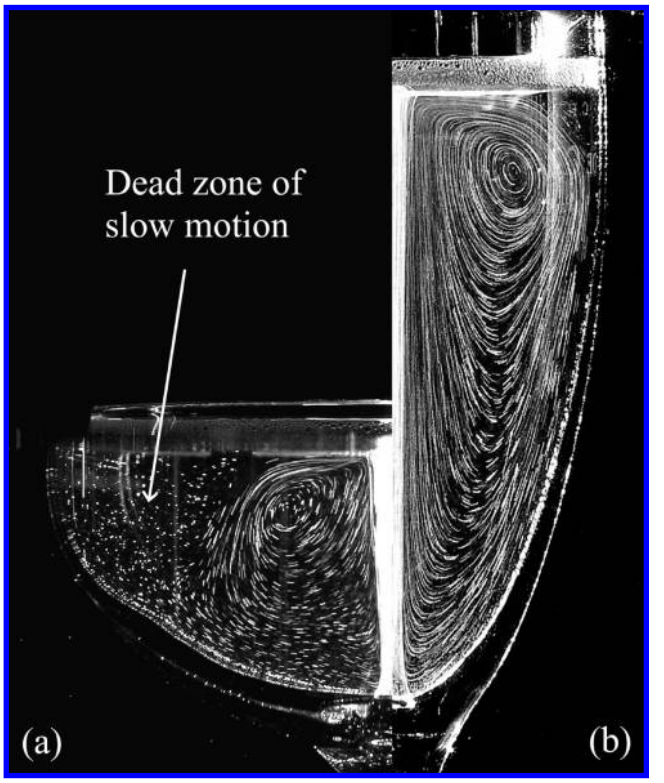

Figure 10. Large-scale flow patterns, driven by the ascending central bubble column, found inside the coupe (**a**) and the flute (**b**), respectively, as seen through laser tomography techniques. Because the flow patterns inside the flute and coupe are axisymmetrical with regard to the central bubble column (*7*−*9*), only half of the flute and coupe are presented to enable a better comparison between the flow patterns found in each type of drinking vessel.

ACKNOWLEDGMENT

Thanks are due to Champagne Pommery for regularly supplying various Champagne samples.

LITERATURE CITED

(1) Liger-Belair, G. *Uncorked: The Science of Champagne*; Princeton University Press: Princeton, NJ, 2004.

(2) Liger-Belair, G. The physics and chemistry behind the bubbling properties of champagne and sparkling wines: a state-of-the-art review. *J. Agric. Food Chem*. **2005**, *53*, 2788–2802.

(3) Liger-Belair, G.; Polidori, G.; Jeandet, P. Recent advances in the science of champagne bubbles. *Chem. Soc. Rev*. **2008**, *37*, 2490–2511.

(4) Shafer, N. E.; Zare, R. N. Through a beer glass darkly. *Phys. Today* **1991**, *44*, 48–52.

(5) Zare, R. N. Strange fizzical attraction. *J. Chem. Educ*. **2005**, *82*, 673–674.

(6) http://www.stanford.edu/group/Zarelab/guinness/.

(7) Liger-Belair, G.; Religieux, J.-B.; Fohanno, S.; Vialatte, M.-A.; Jeandet, P.; Polidori, G. Visualization of mixing flow phenomena in champagne glasses under various glass-shape and engravement conditions. *J. Agric. Food Chem*. **2007**, *55*, 882–888.

(8) Liger-Belair, G.; Beaumont, F.; Vialatte, M.-A.; Jégou, S.; Jeandet, P.; Polidori, G. Kinetics and stability of the mixing flow patterns found in champagne glasses as determined by laser tomography techniques: likely impact on champagne tasting. *Anal. Chim. Acta* **2008**, *621*, 30–37.

(9) Polidori, G.; Beaumont, F.; Jeandet, P.; Liger-Belair, G. Visualization of swirling flows in champagne glasses. *J. Visualization* **2008**, *11*, 184.

(10) Tsachaki, M.; Gady, A.-L.; Kalopesas, M.; Linforth, R.; Athès, V.; Marin, M.; Taylor, A. Effect of ethanol, temperature and gas flow rate on volatile release from aqueous solutions under dynamic headspace dilution conditions. *J. Agric. Food Chem*. **2008**, *56*, 5308–5315.

(11) Liger-Belair, G.; Villaume, S.; Cilindre, C.; Jeandet, P. Kinetics of CO_2 fluxes outgassing from champagne glasses in tasting conditions: the role of temperature. *J. Agric. Food Chem*. **2009**, *57*, 1997–2003.

(12) Mulier, M.; Zeninari, V.; Joly, L.; Decarpenterie, T.; Parvitte, B.; Jeandet, P.; Liger-Belair, G. Development of a compact CO_2 sensor based on near-infrared technology for enological applications. *Appl. Phys. B, Lasers Opt*. **2009**, *94*, 725–733.

(13) Liger-Belair, G. Nucléation, ascension et éclatement d'une bulle de champagne. *Ann. Phys. (Paris)* **2006**, *31*, 1–133.

(14) Liger-Belair, G.; Beaumont, F.; Jeandet, P.; Polidori, G. Flow patterns of bubble nucleation sites (called fliers) freely floating in champagne glasses. *Langmuir* **2007**, *23*, 10976–10983.

(15) Dioxyde de Carbone Ref MA-F-AS314-01-DIOCAR. In *Recueil des méthodes internationales d'analyses des boissons spiritueuses, des alcools et de la fraction aromatique des boissons*; Office International de la Vigne et du Vin: Paris, France, 1994.

(16) Liger-Belair, G.; Rochard, J. *Les vins Effervescents*; Dunod: Paris, France, 2008.

(17) Priser, C.; Etievant, P. X.; Nicklaus, S.; Brun, O. Representative Champagne wine extracts for gas chromatography olfactometry analysis. *J. Agric. Food Chem*. **1997**, *45*, 3511–3514.

(18) Tominaga, T.; Guimbertau, G.; Dubourdieu, D. Role of certain volatile thiols in the bouquet of aged Champagne wines. *J. Agric. Food Chem*. **2003**, *51*, 1016–1020.

(19) Liger-Belair, G.; Voisin, C.; Jeandet, P. Modeling non-classical heterogeneous bubble nucleation from cellulose fibers: application to bubbling in carbonated beverages. *J. Phys. Chem. B* **2005**, *109*, 14573–14580.

(20) Liger-Belair, G.; Parmentier, M.; Jeandet, P. Modeling the kinetics of bubble nucleation in champagne and carbonated beverages. *J. Phys. Chem. B* **2006**, *110*, 21145–21151.

(21) Zhang, Y.; Xu, Z. Fizzics of bubble growth in beer and champagne. *Elements* **2008**, *4*, 47–49.

(22) Zhang, Y.; Xu, Z. Kinetics of convective crystal dissolution and melting, with applications to methane hydrate dissolution and dissociation in seawater. *Earth Planet. Sci. Lett*. **2003**, *213*, 133–148.

(23) Zhang, Y. *Geochemical Kinetics*; Princeton University Press: Princeton, NJ, 2008.

(24) Incropera, F.; Dewitt, D.; Bergman, T.; Lavine, A. *Fundamentals of Heat and Mass Transfer*; Wiley: New York, 2007.

Received March 10, 2009. Revised Manuscript Received April 7, 2009. Thanks are due to the Europôl'Agro Institute and to the Association Recherche Oenologie Champagne Université for financial support. We are also indebted to the Région Champagne-Ardenne, the Ville de Reims, and the Conseil Général de la Marne for supporting our research.